The Design of a Stereo Panorama Camera for Scenes of Dynamic Range

Shou-Kang Wei, Fay Huang, and Reinhard Klette
CITR, Computer Science Department,
The University of Auckland, Auckland, New Zealand
{shoukang, fay, rklette}@citr.auckland.ac.nz

Abstract

Existing stereo panorama cameras do not allow controllability of pictorial/scene composition and stereo acuity (depth levels) over dynamic 3D scene ranges. We specify the design of such a camera allowing this type of flexibility. Previous approaches to design panorama cameras even lack studies with respect to this important aspect, while other design issues such as epipolar geometry, optics optimization, or realization-oriented approximations have been investigated. Without incorporating the controllability into stereo panorama camera design, the poor quality of produced stereo panoramas is foreseeable (e.g. incoherence, cardboard-effect, dipopia etc).

The paper proposes a solution to incorporate controllability into previously discussed [3, 8, 7, 5] stereo panorama camera models. By using a stereo panorama camera equipped with the designed camera parameters according to our solution, the desired/expected pictorial composition and stereo acuity in resultant stereo panoramas can be ensured.

1. Introduction

Stereo panoramas have been found very useful in the applications of immerse technology, telepresence, robot navigation, localization etc [3, 10, 4, 8, 2].

Traditionally the design of stereo panorama cameras is mainly concerned with epipolar geometry, optics optimization, or some other realization/practical issues [3, 7, 5, 1, 6, 9]. This paper draws attention to two further criteria of stereo panorama camera design: controllabilities of pictorial/scene composition and stereo acuity (depth levels) over certain dynamic 3D scene ranges. Lacks of either capabilities result in difficulties in camera positioning, which causes unnecessary consumption of time and costs; and/or poor stereo quality such as cardboard-effects, dipopia etc. in resultant images for intended ranges of 3D scenes.

The paper focuses on the problem how the proposed controllabilities can be realized for previously suggested [3, 8, 7, 5] architectures of stereo panorama cameras.

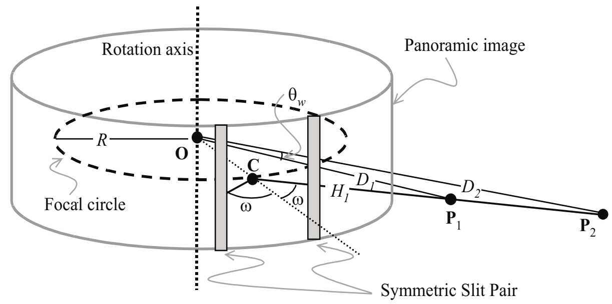

Figure 1. Camera and scene range models.

2. Basic Geometry

The geometry of a stereo panorama camera and parameters, crucial for camera analysis, are depicted in Fig. 1. Due to the dynamic ranges of 3D scenes, a stereoscopic imaging system must be equipped with certain flexibility and controllability so that constraints posed by the application (e.g. pictorial composition or stereo acuity) can be satisfied.

Two main camera parameters providing such a flexibility/controllability are: (1) the distance between the line camera's focal point **C** and the rotation axis, denoted as R; and (2) the angle between a normal vector of the focal circle[1] at the associated focal point and the optical axis of the line camera, denoted as ω. A panoramic pair of ω and $(360° - \omega)$ is referred to as a *symmetric pair* [1]. An important property of such a symmetric pair is that epipolar lines are image rows (see proof in [1]) simplifying stereo analysis.

Concentric cylinders define a scene model coherent with 360° panoramas. Each cylinder represents a particular scene range characterized by its radius, which serve as scene range descriptors. We denote them as D_1 and D_2 and assume $D_1 < D_2$.

[1]A focal circle is the path of all focal points during rotation.

Furthermore, we introduce two application-specific parameters, which are useful for the study of stereo panorama cameras: (1) the distance, denoted as H_1, between camera focal point **C** and target range of scene objects of interest (e.g. $\mathbf{P}_1$ in Fig. 1); and (2) the width of the angular disparity interval, denoted as θ_w, defined by the difference between minimum and maximum angular disparities[2] in a resultant stereo panoramic pair. The parameter H_1 influences the pictorial composition via a 'factoring' of the vertical field of view. The parameter θ_w determines stereo acuity. Both parameters can be used in image acquisition to formulate constraints for the relations between camera-specific parameters and scene range descriptors, and are usually calculated by the application requirement.

Note that the parameters introduced can all be orthographically projected onto the camera's focal plane on which all the camera's focal points lie. Without loss of validity, the following studies/analyses are presented in two-dimensional space.

3. Problem Statement

The specifications of application requirements for stereo panorama image acquisition can be described by intervals of scene range descriptors and application-specific parameters. Formally, we define them as $[D_{1min}, D_{1max}]$, $[D_{2min}, D_{2max}]$, $[H_{1min}, H_{1max}]$, and $[\theta_{wmin}, \theta_{wmax}]$, where $D_{1max} < D_{2min}$.

In theory, the value of R can be any positive real and the value of ω can be any positive real less than $360°$. Practically, motivated by system realization or cost issues, the intervals of both parameters should be as small as possible for a given application.

Without loss of generality, let $R_{min} = \omega_{min} = 0$, and consider the problem of finding minimum values of R_{max} and ω_{max} that fully satisfy the specifications of application requirements.

4. Analysis

Geometrically for each of parameters R and ω the problem consists in finding the maximum value in a bounded four-dimensional space. It is difficult to imagine such a hyper-surface in a five-dimensional space. To understand the behavior of such a hyper-surface in our case, we analyze individual relations between values of R and ω and values of all other camera parameters.

In Fig. 2, we illustrate how the values of R and ω change as the value of one of the scene parameters changes while all others remain constant. In each drawing, we only show a few states of the particular variable to demonstrate the changing behaviors of R and ω values. In each case, if different constant values are chosen, only the magnitudes of the R and ω values will change accordingly, but the 'behaviors' of their changes will remain the same.

[2] *Angular disparity* is defined by the angle between two rays, starting at rotation center **O** and passing through a pair of corresponding projections of a 3D point.

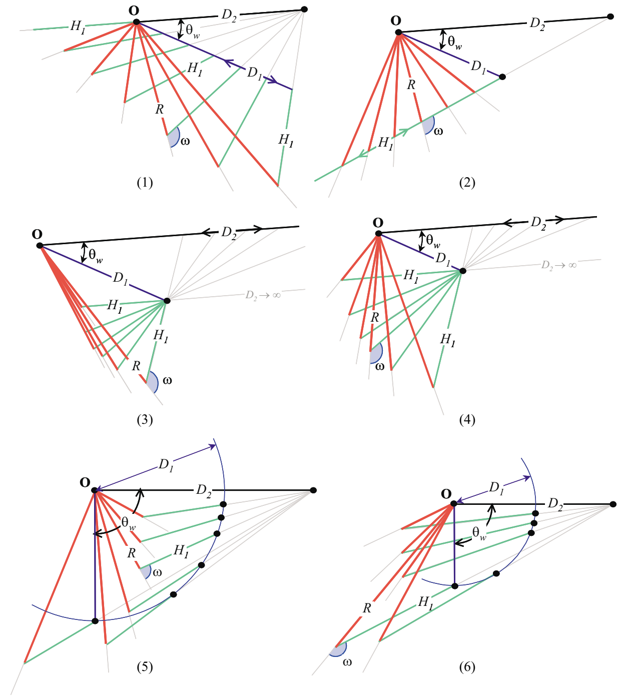

Figure 2. Analysis of the geometric relations.

4.1. D_1 vs. R and ω

For some constant values of D_2, H_1, and θ_w, the geometry of a change of the D_1 value versus changes in R and ω values is visualized in Fig. 2(1). From such geometric studies we conclude the following:

(i) we have $\lim_{D_1 \to 0^+} R = H_1$ and $\lim_{D_1 \to 0^+} \omega = 180°$;

(ii) we have

$$\lim_{D_1 \to D_2^-} R = \sqrt{D_2^2 + H_1^2 + 2D_2H_1 \sin\left(\frac{\theta_w}{2}\right)}, \text{ and}$$

$$\lim_{D_1 \to D_2^-} \omega = \arccos\left(\frac{-H_1 - D_2 \sin\left(\frac{\theta_w}{2}\right)}{\sqrt{D_2^2 + H_1^2 + 2D_2H_1 \sin\left(\frac{\theta_w}{2}\right)}}\right);$$

(iii) by (i) and (ii), we know that $\lim_{D_1 \to 0^+} R < \lim_{D_1 \to D_2^-} R$ and $\lim_{D_1 \to 0^+} \omega > \lim_{D_1 \to D_2^-} \omega$;

and these relations are valid for any given values of D_2, H_1, and θ_w. For all the values of D_1 in interval (0, D_2), it also follows that there exist values of R and ω less than the limits calculated above respectively.

4.2. H_1 vs. R and ω

For some constant values of D_1, D_2, and θ_w, the geometry of changing the H_1 value versus changes in R and ω values is visualized in Fig. 2(2). From these geometric studies it follows:

(i) we have $\lim_{H_1\to 0^+} R = D_1$ and

$$\lim_{H_1\to 0^+} \omega = \arccos\left(\frac{D_2\cos(\theta_w) - D_1}{\sqrt{D_1^2 + D_2^2 - 2D_1D_2\cos(\theta_w)}}\right);$$

(ii) we have $\lim_{H_1\to\infty} R = \infty$ and $\lim_{H_1\to\infty} \omega = 180°$;

and these relations are valid for any given values of D_1, D_2, and θ_w. For all the values of H_1 in $(0, \infty)$, it also follows:

(i) there exist values of R less than $\lim_{H_1\to 0^+} R$;
(ii) the value of ω increases/decreases while the value of H_1 increases/decreases.

4.3. D_2 vs. R and ω

Figure 2(3) and (4), show the geometry of changing the D_2 value versus changes in R and ω values when the values of D_1, H_1, and θ_w are kept constant. In (3) we have the case when $D_1 \geq H_1$, and in (4) we have $D_1 < H_1$. For any given values of D_1, H_1, and θ_w, we have

$$\lim_{D_2\to D_1^+} \omega = \arccos\left(\frac{-H_1 - D_1\sin\left(\frac{\theta_w}{2}\right)}{\sqrt{D_1^2 + H_1^2 + 2D_1H_1\sin\left(\frac{\theta_w}{2}\right)}}\right),$$

and

$$\lim_{D_2\to\infty} \omega = 180° - \arccos\left(\frac{H_1 - D_1\cos(\theta_w)}{\sqrt{D_1^2 + H_1^2 - 2D_1H_1\cos(\theta_w)}}\right).$$

All values of D_2 in (D_1, ∞) satisfy the following relations:

(i) In both cases, the value of R increases/decreases while the value of D_2 decreases/increases.
(ii) In case (3), the value of ω increases/decreases while the value of D_2 decreases/increases.
(iii) In case (4), there exist values of ω less than both $\lim_{D_2\to D_1^+} \omega$ and $\lim_{D_2\to\infty} \omega$.

4.4. θ_w vs. R and ω

The valid value of θ_w is defined to be in the open interval $(0°, 90°)$. Figure 2(5) and (6) show the geometry of changing the θ_w value versus changes in R and ω values when the values of D_1, D_2, and H_1 are kept constant. In (5) we have the case that $D_1 \geq H_1$, and in (6) we have $D_1 < H_1$. These geometric studies prove:

(i) in case (5), we have $\lim_{\theta_w\to 0^+} \omega = 0°$, and in case (6), we have $\lim_{\theta_w\to 0^+} \omega = 180°$;
(ii) in both cases, we have

$$\lim_{\theta_w\to 90^-} \omega = \arccos\left(\frac{-D_1^2}{\sqrt{A(D_1^2 + H_1^2) + 2D_1^2H_1\sqrt{A}}}\right),$$

where $A = (D_1^2 + D_2^2)$;

for any given values of D_1, D_2, and H_1. For all the values of θ_w in $(0°, 90°)$ it follows:

(i) in both cases, the value of R increases/decreases while the value of D_2 increases/decreases;
(ii) in case (5), the value of ω increases/decreases while the value of D_2 increases/decreases;
(iii) in case (6), there exist values of ω less than both $\lim_{\theta_w\to 0^+} \omega$ and $\lim_{\theta_w\to 90^-} \omega$.

5. Camera Parameters Design

This section explains how the camera parameters R and ω are designed using previous analysis results.

The individual graphs of R and ω with respect to each of the parameters D_1, H_1, D_2, and θ_w are shown in Fig. 3. All graphs illustrate the general behavior of how the values of R and ω change while just one of the values of D_1, H_1, D_2, and θ_w varies.

Let functions $f_1(D_1)$, $f_2(H_1)$, $f_3(D_2)$, and $f_4(\theta_w)$ be defined to be the value of R with respect to the single variable D_1, H_1, D_2, and θ_w respectively. Similarly, functions $f_5(D_1)$, $f_6(H_1)$, $f_7(D_2)$, and $f_8(\theta_w)$ are defined to be the value of ω following the same convention. All of them are continuous functions.

Both functions $f_1(D_1)$ and $f_2(H_1)$ have a single minimum, and their graphs are concave upward on $(0, D_2)$ and $(0, \infty)$ respectively. Functions $f_3(D_2)$ and $f_4(\theta_w)$ are decreasing on (D_1, ∞) and $(0°, 90°)$ respectively. Function $f_5(D_1)$ has a single minimum on $(0, D_2)$. Function $f_6(H_1)$ is increasing on $(0, \infty)$. Moreover, in the case of $D_1 \geq H_1$, function $f_7(D_2)$ is decreasing on (D_1, ∞). On the other hand, in the case of $D_1 < H_1$, function $f_7(D_2)$ has a single minimum on (D_1, ∞). Finally, in the case of $D_1 \geq H_1$, function $f_8(\theta_w)$ is increasing on $(0°, 90°)$. For the case of $D_1 < H_1$, function $f_8(\theta_w)$ has a single minimum on $(0°, 90°)$.

Since all the graphs of functions f_1, f_2, f_3, and f_4 are decreasing, increasing or concave upward, we may conclude that the maximum value of R within the bounded region defined by intervals $[D_{1min}, D_{1max}]$, $[D_{2min}, D_{2max}]$, $[H_{1min}, H_{1max}]$, and $[\theta_{wmin}, \theta_{wmax}]$ lies on the boundary of the region. This reduces the search space for the maximum of R from a four-dimensional bounded space down to

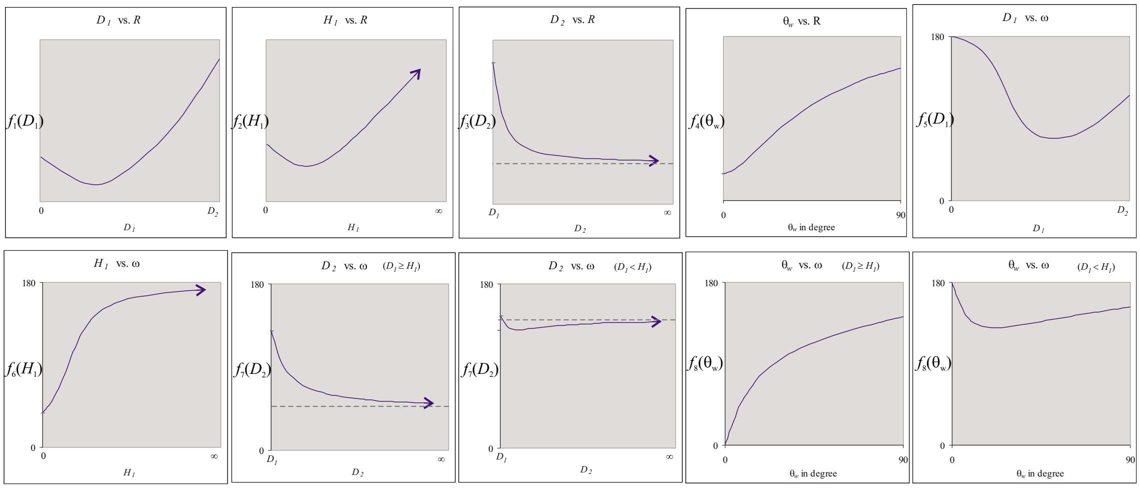

Figure 3. The graphs of R and ω with respect to each of the parameters.

16 (check/search) points, i.e. all possible combinations of these boundary values.

Furthermore, since function $f_3(D_2)$ is decreasing, the maximum value of R exists when D_2 equals to D_{2min}. Since $f_4(\theta_w)$ is an increasing function, the maximum value of R exists when θ_w equals to $\theta_{w max}$. From these results, we may conclude that the search space of 16 points can be further reduced to four to find the maximum value of R, i.e. the minimum R for intervals defined by application-specific requirements.

Similar to functions f_1, f_2, f_3, and f_4 all the graphs of functions f_5, f_6, f_7, and f_8 are decreasing, increasing or continuous and have a single minimum, we may again conclude that the maximum value of ω also lies on the boundary of the region. This reduces the search space for the maximum of ω to also 16 (check/search) points.

Seeing as $f_6(H_1)$ is an increasing function, the maximum value of ω exists when H_1 equals to H_{1max}. This further reduces the search space from 16 points to eight for finding the maximum value of ω. Moreover, if $D_{1min} \geq H_{1max}$, then only one comparison between two values is sufficient to find the maximum value of ω. Alternatively, if $D_{1min} \leq H_{1max} \leq D_{1max}$, then the cardinality of our search space is just five.

6. Conclusions

The acquisition of stereo panoramas requires dynamic adjustments for different scene ranges. Stereo panoramic camera design should incorporate such commonly demanded functions such that high quality of produced stereo panoramas for dynamic ranges of scenes can be achieved. This paper addressed a novel approach to camera parameter design for an already known (and commercially available) architecture of stereo panorama cameras, and ensures that the requirements of desired pictorial compositions and stereo acuity over specified dynamic scene ranges are attainable. Moreover, our approach contributes to the design process for camera parameters by reducing the search space drastically from a four-dimensional bounded set to seven comparisons at most.

References

[1] F. Huang, S. K. Wei, and R. Klette. Geometrical fundamentals of polycentric panoramas. In *Proc. ICCV'01*, pages 560–565, Vancouver, Canada, July 2001.
[2] H.-C. Huang and Y.-P. Hung. Panoramic stereo imaging system with automatic disparity warping and seaming. *GMIP*, 60(3):196–208, 1998.
[3] H. Ishiguro, M. Yamamoto, and S. Tsuji. Omni-directional stereo. *PAMI*, 14(2):257–262, 1992.
[4] S.-B. Kang and P. Desikan. Virtual navigation of complex scenes using clusters of cylindrical panoramic images. Technical Report Technical Report CRL 97/5, Digital Equipment Corporation, Cambridge Research Lab, WhereUnknown, September 1997.
[5] S. Peleg, Y. Pritch, and M. Ben-Ezra. Cameras for stereo panoramic imaging. In *Proc. CVPR'00*, pages 208–214, Hilton Head Island, Jime 2000.
[6] S. M. Seitz. The space of all stereo images. In *Proc. ICCV'01*, pages 26–33, Vancouver, Canada, July 2001.
[7] H. Shum, A. Kalai, and S. Seitz. Omnivergent stereo. In *Proc. ICCV'99*, pages 22–29, Korfu, Greece, September 1999.
[8] S.-K. Wei, F. Huang, and R. Klette. Three-dimensional scene navigation through anaglyphic panorama visualization. In *Proc. CAIP'99 (LNCS 1689)*, pages 542–549, Ljubljana, Slovenia, September 1999.
[9] T. Werner and T. Pajdla. Cheirality in epipolar geometry. In *Proc. ICCV'01*, pages 548–553, Vancouver, Canada, July 2001.
[10] J.-Y. Zheng and S. Tsuji. Panoramic representation for route recognition by a mobile robot. *IJCV*, 9(1):55–76, 1992.